JOURNAL OF GEOPHYSICAL RESEARCH, VOL. 91, NO. A3, PAGES 3077–3088, MARCH 1, 1986

Relativistic Electron and Energetic Ion Precipitation Spikes Near the Plasmapause

W. L. IMHOF, H. D. VOSS, J. B. REAGAN, D. W. DATLOWE, E. E. GAINES, AND J. MOBILIA

Lockheed Palo Alto Research Laboratory, Palo Alto, California

D. S. EVANS

National Oceanic and Atmospheric Administration, Boulder, Colorado

An investigation has been made of electron and associated ion precipitation spikes near the plasmapause that are narrow in L shell and in which relativistic electrons are favored. The electron energy spectra during the spikes sometimes had equivalent e fold energies in excess of 500 keV. In approximately 31% of these spike events observed from the low-altitude polar orbiting satellites P72-1, P78-1, and S81-1, nearly simultaneous precipitation was measured in energetic ions above ~30 keV at about the same L value. Several of the precipitation spikes occurred primarily in the drift loss cone, but in some cases, significant precipitation ($\sim 10^{-2}$ ergs/cm^2 s) was also observed in the bounce loss cone. The electron spikes occurred preferentially in the evening sector, and all of the associated narrow ion spikes were in that local time interval. Narrow relativistic electron spikes were observed on less than 1% of the crossings of the plasmapause. From the set of S81-1 events a search was made for those also observed on the NOAA 6 spacecraft. On rare occasions, nearly simultaneous (<2000 s) narrow spikes with hard electron spectra were found at approximately the same L value from both spacecraft and at longitudes differing by 8°–47°. These findings suggest a patchy profile, sometimes with an arc structure which may extend over longitude intervals as great as 25° and time intervals as long as 2000 s. From consideration of the AE index for 17 events, 12 were found to occur close to the times of substorms. The spike precipitation is interpreted in terms of cyclotron resonance wave-particle interactions involving radiation belt particles, the narrow widths being associated with fine structure in the cold plasma density profiles near the plasmapause and the energy selectivity associated with an upper frequency cutoff in the waves.

INTRODUCTION

The possibility that relativistic electrons can undergo a cyclotron resonance with electromagnetic ion cyclotron waves that are associated with proton precipitation was first suggested by *Thorne and Kennel* [1971]. They indicated that relativistic electron precipitation may be parasitic, i.e., driven by waves generated by the precipitation of ring current protons. One of the predictions of this mechanism is that relativistic electron precipitation should be correlated with more intense low-energy (5–50 keV) proton precipitation fluxes along the bulge region of the plasmapause. However, such precipitation processes may only apply to highly relativistic electrons when finite temperatures are considered, as shown by *Davidson* [1978].

Relativistic electron precipitation phenomena in conjunction with ion precipitation might best be studied when confined to a narrow latitude interval. Narrow L shell bands of electron precipitation in the outer radiation belt were reported by *Koons et al.* [1972], and simultaneous wave measurements indicated that the electrons were pitch angle scattered in the presence of intense ELF electrostatic waves. The precipitating electrons were several hundred keV in energy, but associated proton measurements were not presented. Narrow zones of preferentially relativistic electron precipitation were first reported by *Imhof et al.* [1977], but no attempt was made to correlate the phenomenon with ion precipitation. Relativistic electron precipitation events that occur over a narrow latitudinal zone embedded within a broader region of intense energetic ion precipitation were presented by *Thorne and Andreoli* [1980]. In that study, four events were found with a well-defined threshold energy for electron precipitation which they attributed to electromagnetic ion cyclotron waves. Single and multiple peaks in precipitating protons of >120 keV having a narrow distribution in L above a smooth continuum were reported by *Reagan et al.* [1975]. Spiky structures in proton precipitation were also observed by *Koons* [1975].

In the present paper we specifically address only events involving the preferential precipitation of high-energy electrons over a narrow range in L shell and look for associated ion precipitation in those events. We avoid the preferential high-energy precipitation near the trapping boundary, which often displays hard spectra with shapes that vary strongly with L [*Imhof et al.*, 1979]. In addition to finding nearly simultaneous ion precipitation during two of the relativistic electron events previously published by *Imhof et al.* [1977], we report the results of a study of this class of events with data acquired on the P78-1, the S81-1, and the NOAA 6 spacecraft. From the data presented it is concluded that many of the spikes may have resulted from wave-particle interactions between radiation belt particles and low-frequency waves. The narrowness of the spikes may be associated with fine structure in the cold plasma densities near the plasmapause where many of the events occurred.

DESCRIPTION OF THE INSTRUMENTATION

In this paper, use is made of data acquired on four polar orbiting satellites. The pertiment instrumentation in each of these is listed in Table 1. In the data analysis, L values were calculated using the Goddard Space Flight Center (GSFC 12/66) geomagnetic field model [*Cain et al.*, 1967] for the epoch 1972 (P72-1 data) or the epoch 1980 (P78-1, S81-1, and NOAA 6).

Paper number 5A8827.
0148-0227/86/005A-8827$05.00

TABLE 1. Electron/Proton Detectors

Satellite				Particle Detectors					
Name	Altitude, km	Local Time	Spinning (Period) or Oriented	Name	Type	Threshold Energy	Geometric Factor, cm^2 sr	Acceptance Angle, deg	Mirroring or Precipitating
P72-1	736–761	Noon, midnight	Spinning (5 s)	EEM 001	Electrons	160 keV	0.36	±20	Both
				LEP 001	Ions	120 keV	0.09	± 8	Both
				Anti for Ge spectrometer	Electrons	3–4 MeV	···	Omni	Both
P78-1	550–625	Noon, midnight	Spinning (5.5 s)	EEM 002	Electrons	68 keV	0.69	±15	Both
				LEP 002	Ions	60 keV	0.1	± 16	Both
				Anti for Ge spectrometer	Electrons	3–4 MeV	···	Omni	Both
S81-1	170–280	1030, 2230	Oriented	ME 1	Electrons	45 keV	2.47	±30	Precipitating (zenith)
				TE 2	Electrons	6 keV	0.17	±20	Mirroring (90° to zenith)
				LE 4	Ions	50 keV	0.1	±10	Both (50° to zenith)
				Anti for ME 1 spectrometer	Electrons	1–6.5 MeV	···	Omni	Both
NOAA 6	800–830	0730, 1930	Oriented	Electron spectrometer	Electrons	30 keV	0.0095	±15	Precipitating (zenith)
				Electron spectrometer	Electrons	30 keV	0.0095	±15	Mirroring (81° to zenith)
				Proton spectrometer	Protons	30 keV	0.0095	±15	Precipitating (zenith)
				Proton spectrometer	Protons	30 keV	0.0095	±15	Mirroring (83° to zenith)

All of the particle spectrometers contained silicon solid state sensors except for the EEM 001 instrument, which consisted of a plastic scintillator. Each provided energy spectral information through pulse height analysis. The electron spectrometers on the P72-1 and P78-1 spacecraft are described by *Imhof et al.* [1979] and *Imhof et al.* [1981], respectively. The proton spectrometer on the P72-1 satellite was described by *Reagan et al.* [1975]. Each of the payloads on the P72-1 and P78-1 satellites also contained large-volume anticoincidence scintillator shields which responded to electrons above a relatively high threshold energy. These anticoincidence counters provided no spectral information but had a high sensitivity and were therefore suitable for detecting relativistic electron precipitation spikes. The anticoincidence counter surrounding the Germanium spectrometer on the P72-1 satellite consisted of a plastic scintillator and is described by *Nakano et al.* [1974], whereas those in the Germanium spectrometers on the P78-1 spacecraft consisted of sodium iodide (polyscin) and are described by *Nakano et al.* [1980].

The payload in the SEEP (Stimulated Emission of Energetic Particles) experiment on the S81-1 spacecraft contained an array of cooled silicon solid state detectors to measure electrons and ions directly with high-sensitivity and fine energy resolution [*Voss et al.*, 1982]. The anticoincidence counter surrounding the ME 1 spectrometer consisted of a plastic scintillator.

The Space Environment Monitor on the NOAA 6 satellite includes a set of silicon solid state detectors which measure the intensity of electrons and ions above 30 keV. Two electron and two proton detector systems are mounted in pairs, one of each type oriented to view zenith, the other two viewing at 83° (protons) and 81° (electrons) to the first pair in a plane perpendicular to the orbit plane. For the events studied here the detector pair which viewed zenith was measuring precipitating particles, whereas the other pair detected particles with local pitch angles near 90°.

PRESENTATION OF DATA

Examples of Events Observed From Single Spacecraft

Data from three satellites, P72-1, P78-1, and S81-1, were individually surveyed to find narrow spikes (less than 10 s observing time) in the fluxes of electrons above energies of ~4 MeV, ~3.5 MeV, or 1–6.5 MeV, respectively. The number of events was 9, 8, and 24, from 8, 14, and 7 months of survey in 1972–1973, 1979–1980, and 1982, respectively. In all cases the selection criteria required that the flux enhancements were not associated with the isotropic pitch angle distribution commonly present at the trapping boundary.

The narrow energy selective electron precipitation events reported here are uncommon in that only 41 events in the P72-1, P78-1, and S81-1 data were found from a survey of many orbits. A quantitative assessment of the frequency of onset of events and intercomparisons between the occurrence rates observed by the vehicles during various time periods is limited by the unavoidably different event criteria used in each case and the varying portions of the complete data sets that were analyzed. The threshold energies and geometric factors for detecting events in the anticoincidence counters were not the same, and two vehicles (P72-1 and P78-1) were spinning, whereas the S81-1 satellite was oriented. However, one can state that the narrow ($\lesssim$10 s duration in the spacecraft frame) relativistic electron precipitation spikes were observed to occur on less than 1% of the crossings of the plasmapause. Accordingly, this particular class of precipitation does not represent a major contribution to the losses of particles from the radiation belts. However, they are important to study, because the electron and ion precipitation enhancements are often nearly simultaneous and narrow in time or L shell and therefore present a unique opportunity to study the precipitation processes.

Out of the total of 41 narrow energy selective electron precipitation events reported here in the P72-1, P78-1, and S81-1

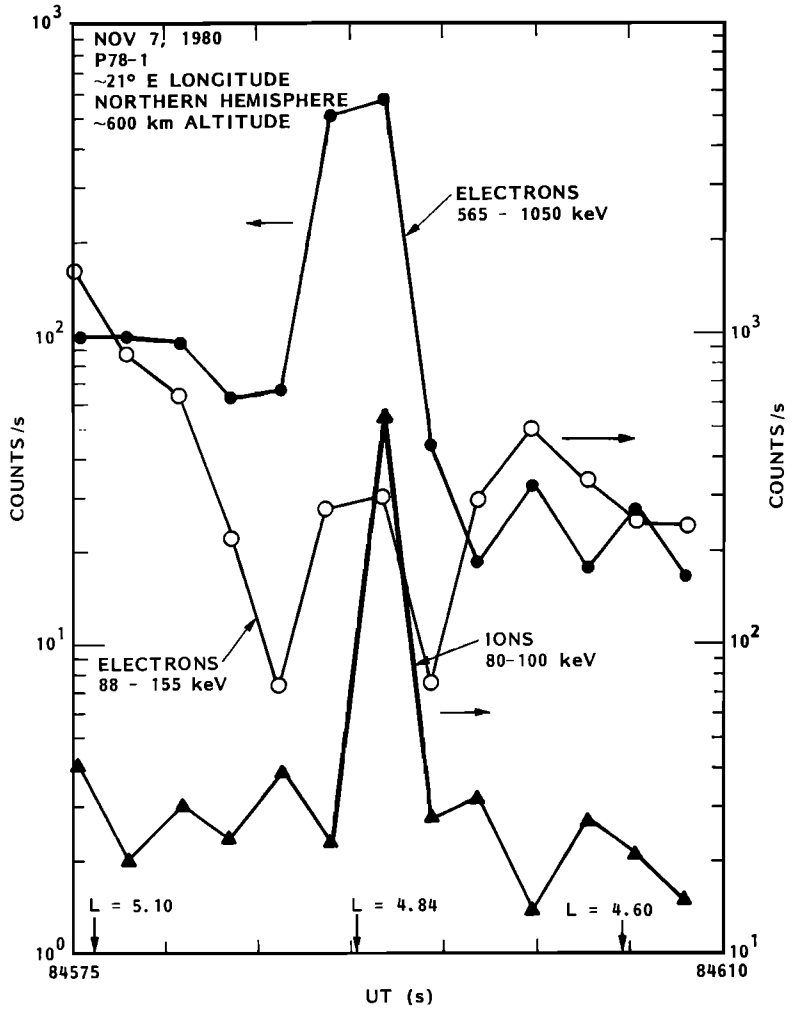

Fig. 1. The counting rates observed with the EEM 002 and LEP 002 spectrometers on the P78-1 satellite for electrons and ions in selected energy intervals and at local pitch angles near 90°. Arrows indicate the applicable vertical scale in each case.

data, nine of these events also contained a narrow zone of energetic ion precipitation at nearly the same time and L shell. However, in these nine cases, small but distinct differences in the observed L shell widths and/or positions were often present. In regard to the frequency of occurrence of simultaneous ion and electron precipitation events it should be realized that in 12 of the 24 S81-1 events the instrumentation was not in a mode suitable for detecting ions. Since these narrow precipitation events are rare, the near-coincidence of 9 out of 29 or 31% of the cases seems to be far more common than accidental. On the other hand, coincident precipitation did not occur in 20 cases, and this might reflect the absence of waves at the appropriate frequency to precipitate the ions.

An example of an event found in the P78-1 data is shown in Figure 1. Here are plotted the average counting rates of locally trapped electrons and ions in selected energy intervals. The high-energy electrons (565–1050 keV) increase by a large factor at ~84590 s UT whereas lower-energy (88–155 keV) electrons show little increase at that time along with a pronounced decrease just before and just afterward. The ions also show a strong spike which is even narrower in time and/or L shell. Most of the particles observed in the event are not directly precipitating in the bounce loss cone, but because of the high B value at their mirror points they will be lost due to atmospheric interactions sometime during their longitude drift around the world. Since the observation point was just a few degrees east of the anomaly in the northern hemisphere, the electrons must have been injected within a few degrees west of the point of observation. The protons, which drift westward, could have been injected far east of the point of observation, but the close agreement with the electron spike makes that seem less likely. Each point in the plot represents the average of approximately twenty-five 0.032-s summation intervals for pitch angles 65°–115° during a half-spin of the satellite. Based on the relative fluxes of the ions and electrons and the observed differences in the flux versus time profiles, it can be shown that the ion enhancements during this and other events cannot be attributed to an instrument response to the higher-energy electrons. Another feature of this event, unlike many of the others, is that the lower-energy electrons showed a pronounced decrease in flux just before and just after the hard spectrum spike.

The preferential enhancement of the higher-energy electrons during the November 7, 1980, event is best illustrated with the energy spectra shown in Figure 2. Here the spectrum during the spike is plotted for comparison with the average of the spectrum before and after the event. Clearly, the higher-energy electrons increased by a much larger factor than did the lower-energy electrons.

An event of the same type was observed by the S81-1 satellite on July 11, 1982. Figure 3 shows the counting rate versus time profile for electrons in the bounce loss cone in two differ-

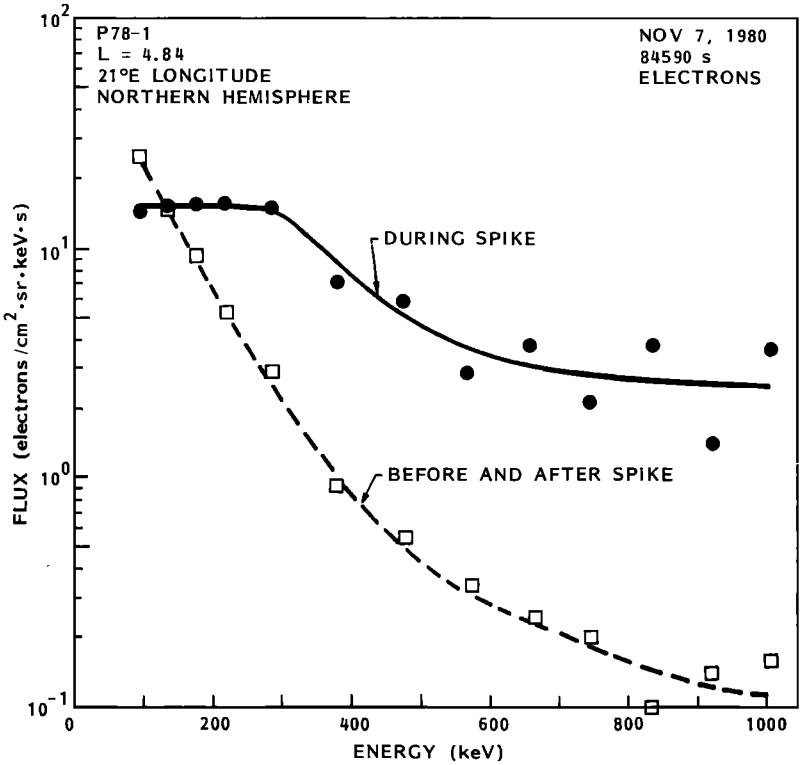

Fig. 2. Energy spectrum measured with the EEM 002 spectrometer during a spike event and the average of that recorded before and after the spike. The channels have been grouped to reduce the statistical uncertainties.

ent energy ranges. As with the pattern of the P78-1 events, the fluxes of electrons of >300 keV increased by a larger factor than did the lower-energy electrons. This tendency is illustrated with the energy spectra measured in ME 1 as shown in Figure 4. One can see that the spectrum is much harder during the spike than before and afterward.

During the event shown in Figure 3 an ion enhancement was observed in the LE 4 spectrometer at nearly the same time as the higher-energy electron flux increase but with a somewhat different time profile and at a slightly different L value. In this regard the event was similar to the one presented in Figure 1 based on the P78-1 data.

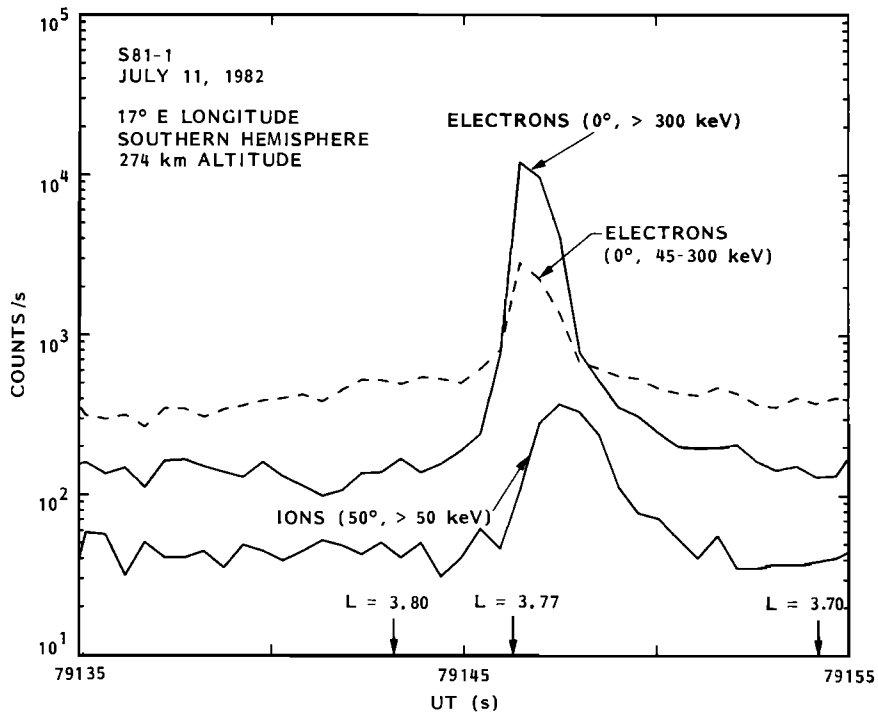

Fig. 3. The counting rates observed with the ME 1 and LE 4 spectrometers in the SEEP payload on the S81-1 spacecraft at local zenith angles of 0° and 50°, respectively, are plotted as a function of time.

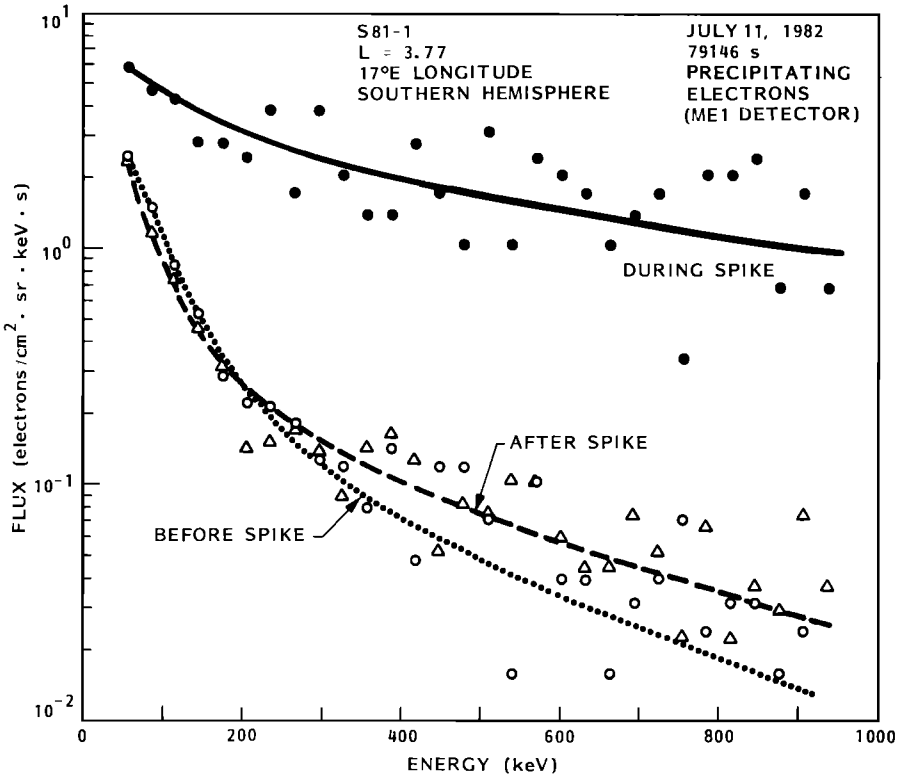

Fig. 4. Energy spectrum measured with the ME 1 spectrometer during a spike event and the spectra recorded before and after the spike. The channels have been grouped to reduce the statistical uncertainties.

Several relativistic electron precipitation spikes over very narrow L shell intervals were previously reported [*Imhof et al.*, 1977] on the basis of data acquired from the P72-1 satellite during an 8-month time period, October 1972 to May 1973. During those events the fluxes of electrons of $\gtrsim$4 MeV underwent pronounced and narrow enhancements lasting less than 10 s, whereas the lower-energy electrons were not significantly affected. Only electrons were considered in the initial study of energy selective precipitation mechanisms using these data. More recently, having observed ion precipitation simultaneously with energy selective electron precipitation in the P78-1 and S81-1 data sets, the older data were examined for the simultaneous occurrence of ion precipitation. On two of the nine events previously studied, narrow zones of ion precipitation were found at nearly the same location on successive orbits. The electron and ion data from these two passes are shown in Figure 5. Clearly, the ions at 250–400 keV show enhanced fluxes over a narrow L shell region at approximately the same time and position as the relativistic electrons with energies of >4 MeV. The close association between the electron and ion spikes makes it less likely that either had been injected far away in longitude and just drifted to the point of observation. From the entire set of on-orbit data as well as the laboratory calibrations it can be shown that the ion spectrometer was not simply responding to relativistic electrons. During the remaining seven relativistic electron precipitation events observed in 1972–1973, narrow and pronounced ion precipitation did not occur, although in some of the cases the ion fluxes were enhanced in the general vicinity of the relativistic electron precipitation.

Events in Both the S81-1 and the NOAA 6 Data

Since the NOAA 6 instrument provided no means of monitoring the fluxes of electrons above energies exceeding 300 keV, a search for relativistic electron precipitation events could not be performed based on the detection of electrons in the MeV range, as done with the P72-1, P78-1, and S81-1 spacecraft. Instead, in the NOAA 6 instruments, electron and proton responses were studied at times within 3 hours of the observation of narrow relativistic electron spikes in the S81-1 spacecraft. The criteria for correlation were further restricted by requiring the NOAA 6 event to be within 60° in longitude and 0.11 units in L value of the S81-1 event.

Examples of relativistic electron precipitation spikes observed in both the S81-1 and NOAA 6 data are shown in Figure 6. In each of the events the spikes consisted of significant enhancements in the fluxes of >300-keV electrons in both the drift and bounce loss cones. The listed angles refer to the zenith viewing directions rather than pitch angles. The central pitch angles for electrons observed by the 0° detectors in the NOAA 6 and S81-1 payloads are all within 27° of being parallel to the magnetic field lines. The pitch angles for the 90° detectors are all within 15° of being perpendicular to the magnetic field lines. On each of these events the fluxes of precipitating electrons above 300 keV increased by larger factors than did those of trapped electrons. Detailed analyses of the precipitating to trapped ratios and comparisons between the NOAA 6 and S81-1 data are limited by an alternation of the 1-s accumulation intervals between the precipitating and trapped particles in the NOAA 6 measurements. In the plots of the latter data the counting rates on successive 1-s intervals are connected by straight lines.

The energy spectra of the precipitating electrons from the S81-1 measurements during the two foregoing events are illustrated in Figure 7. Clearly, the spectra were significantly harder during the spikes than before or after. There is no well-defined energy threshold for flux enhancement, but the fluxes of electrons show a marked increase at energies up to at least 1 MeV. The equivalent e fold energies are sometimes in

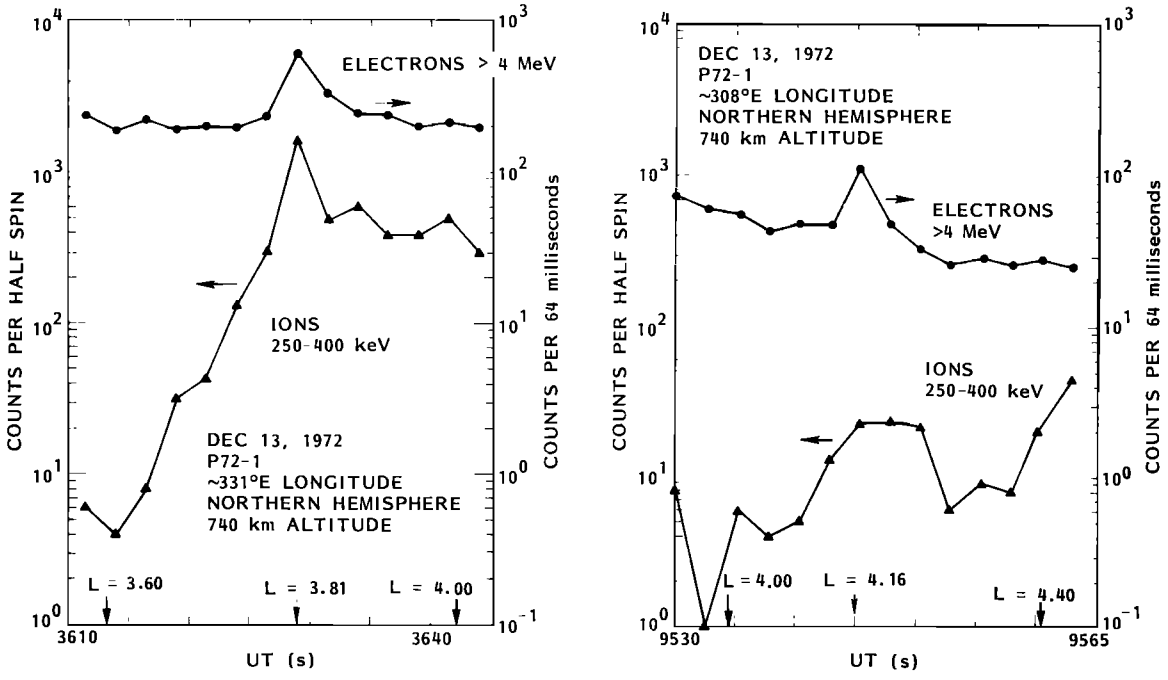

Fig. 5. The counting rate of electrons of >4 MeV observed with the anticoincidence counter surrounding one of the Germanium spectrometers on the P72-1 spacecraft and the rates of ions of 250–400 keV at nearly 90° pitch angle measured in the LEP 001 spectrometer on the same satellite.

excess of 500 keV. During the spikes on September 2, 1982, and November 17, 1982, the energy deposition rates corresponding to the spectra measured in the bounce loss cone were 2.4×10^{-2} and 2.7×10^{-2} ergs/cm^2 s, respectively.

It should be noted that events with large fluxes of high-energy electrons in the bounce loss cone were not observed from the P72-1 and P78-1 satellites, but this measured difference in character of the events may result from the oriented condition of the S81-1 and NOAA 6 experiments in contrast with the spinning nature of the other two satellites and the differences in geometric factors of the various detectors. Also, selecting events observed from two satellites at somewhat different times and positions may have generally favored stronger wave-particle interactions.

Nearly coincident ion spikes appeared in all seven of the NOAA 6 passes in which high-energy electron enhancements occurred at nearly the same L value as in the S81-1 data. However, in two of these events the electron and ion spikes were somewhat wider than 10 s in the spacecraft frame. At the times of these events the ion detector in the S81-1 payload was not in the proper mode for measuring ions, so it is not known whether an ion spike occurred at the time of the SEEP observations. When the S81-1 ion detector was in the correct mode for counting ions and they were detected, corresponding electron spikes in both the S81-1 and the NOAA 6 data were not observed.

The longitude and time differences when similar events were observed in the NOAA 6 and S81-1 data are shown in Figure 8. For all of the plotted points a relativistic electron spike was observed in the S81-1 detector oriented at 0° zenith angle. Different symbols are used to indicate whether or not an electron spike was observed in the NOAA 6 data within 0.11 of the same L value. A shading encompasses electron precipitation events that extend less than 25° in longitude and less than 2000 s in time. Five of seven events observed from both spacecraft fell within these limits. These findings suggest a patchy profile, sometimes with an arc structure which may extend over longitude intervals as great as 25° and time intervals as long as 2000 s. The plot in Figure 8 is consistent with the general lack of occurrence of the energy selective precipitation spikes on successive orbits, differing by ~6000 s in time and about 25° in longitude.

Morphology of the Events

All the narrow electron spikes reported here occurred in the outer radiation belt. The invariant latitude and MLT values are plotted in Figure 9, with different symbols for those that involved only electrons and for those in which the ion fluxes also showed an enhancement. The events are plotted at the local time of observation. Those electrons in the drift loss cone could have been injected at an earlier time, but in most of the cases, electrons are also in the bounce loss cone, and a long longitude drift interval seems less likely. Also shown are the four events presented by *Thorne and Andreoli* [1980] as electromagnetic ion cyclotron wave events. Data coverage on the P72-1 and P78-1 spacecraft was approximately equal near noon and midnight (within about 2 hours), and for the S81-1 satellite it was almost equal near 1030 and 2230 local time (within about 2 hours). At low L values the NOAA 6 measurements covered MLT values of 0630–0900 and 1830–2130. The premidnight hours were clearly the most favored for occurrence of energy selective electron precipitation spikes. This preference was particularly strong for events with nearly simultaneous ion and energy selective relativistic electron precipitation. The concentration of events prior to local midnight is a noteworthy finding, but additional information is needed to establish the source of the spikes.

Since the equatorial plasma densities and hence the wave-particle resonant energies are known to undergo major changes near the plasmapause, it is of interest to consider the locations of these events with respect to that position. In Figure 10 the locations in L of the energy selective spikes are plotted as a function of the position of the plasmapause based on Kp [*Carpenter and Park*, 1973]. This formalism used a

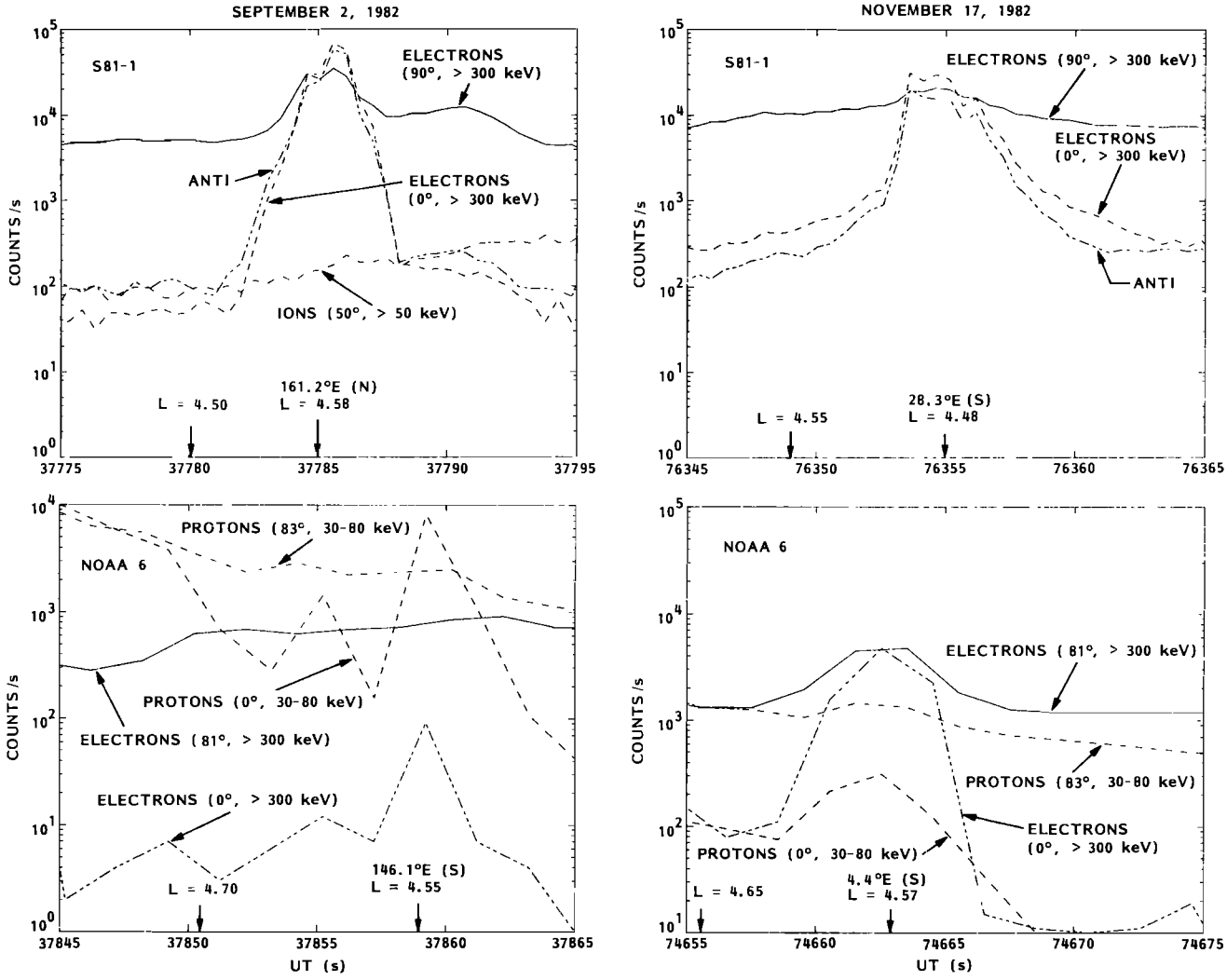

Fig. 6. In the top sections the counting rates observed with ME 1, TE 2, and LE 4 spectrometers in the SEEP payload on the S81-1 spacecraft at local zenith angles of 0°, 90°, and 50°, respectively, are plotted as a function of time for events on (left) September 2, 1982, and (right) November 17, 1982. Also plotted are the counting rates in the anticoincidence counter. In the bottom sections are plotted the counting rates of electrons of >300 keV measured at 0° and at 81° zenith angle and of protons of 30–80 keV measured at 0° and at 83° zenith angle on the NOAA 6 spacecraft. After the longitude values, (N) or (S) indicates whether the observations were made in the northern or southern hemisphere, respectively.

simple dipole model, and consideration of the differences in magnetic field model for the calculation of L value is beyond the scope of this formalism. The formula applies to all magnetic local times, but at MLT values near 2100 the actual L values of the plasmapause may be slightly higher (D. L. Carpenter, private communication, 1985). The L values for the plasmapause location based on the Carpenter and Park formalism are not intended to be accurate representations, but are given mainly to illustrate the general location of the events with respect to the plasmapause position. A Kp scale is provided on the right-hand side. A line is drawn to indicate positions of equal value in L for the spike and the plasmapause. It can be seen that many of the spikes occurred in the vicinity of the plasmapause.

DISCUSSION

It should be emphasized that many of the electron precipitation events reported here were observed in the drift loss cone. Even for the majority of events observed in the bounce loss cone with the S81-1 and NOAA 6 instruments the pitch angle distributions were far from isotropic, with the fluxes near 90° pitch angle often being an order of magnitude greater than those near 0°. In contrast, the energy selective precipitation events reported by *Thorne and Andreoli* [1980] were all measured in the bounce loss cone. The four events with isotropy over the upward looking hemisphere had energy selective properties similar to those reported here. However, those events were discovered from more than 14 months of data, and they occurred in the dusk meridian, a time interval not covered well in the present observations.

The spikes reported by *Koons et al.* [1972] appear similar to those considered in the present paper, but here we have analyzed many electron events and have considered the frequency of occurrence of associated narrow ion spikes. The spikes might also be related to the relativistic electron precipitation (REP) event at $L = 4.5$ reported by *West and Parks* [1984]. Bremsstrahlung X rays and ELF emissions were measured simultaneously. The X ray fluxes had a hard energy spectrum, and the authors concluded they were due to precipitation of relativistic electrons. West and Parks interpreted the event as being the result of electron cyclotron interaction with whistlers. However, the data were limited to one event, so it is

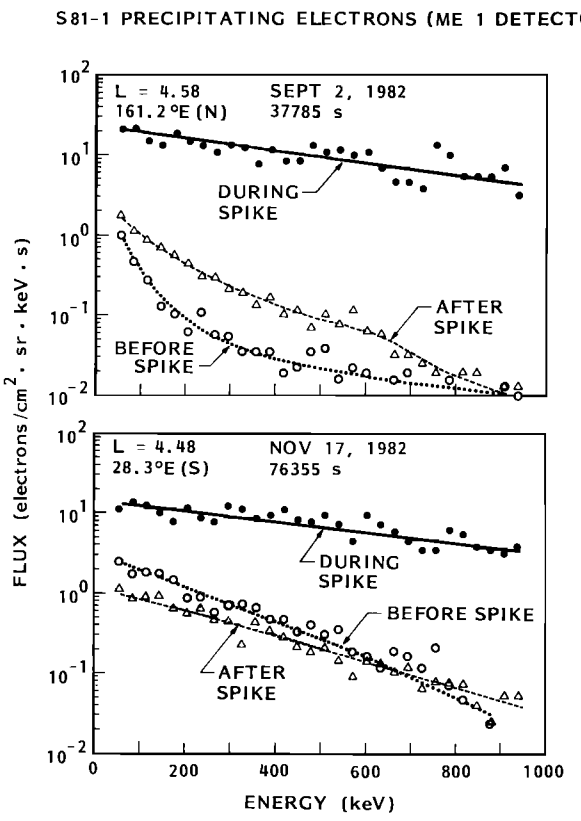

Fig. 7. Energy spectra measured with the ME 1 spectrometer during two different spike events. Also shown are the spectra recorded before and after the spike.

difficult to establish how it might relate to the events presented here.

Many electron and ion precipitation processes are believed to be associated with wave-particle interactions. For simplicity and because a large portion of the length of a field line is near the equator, that region is often taken to be the location where the interactions take place. It is therefore logical to consider the frequencies of the waves that might be responsible for first-order cyclotron resonance at the equator. For this purpose the resonance frequencies were calculated using a program supplied by G. T. Davidson (private communication, 1984). The frequencies for the case on November 7, 1980, are plotted in Figure 11 as a function of the near-equatorial cold plasma density. Cyclotron resonance was assumed for waves traveling parallel to the magnetic field lines, and the wave-particle interactions were all taken to occur at the equator. However, various modes of wave-particle interactions are possible, and therefore the wave frequencies for a given plasma density may be somewhat different than shown. Many of the events occurred in the neighborhood of $L = 4$–5, and the cold plasma densities in the equatorial region were therefore generally in the vicinity of 100 cm^{-3}. The frequencies of the waves responsible for the electron precipitation were probably in the range 10–100 Hz. An upper frequency cutoff in the waves could account for the observed energy selectivity. The nearly simultaneous precipitation of ions would require that the waves extend to lower frequencies, 1 Hz or less. Waves of such low frequencies could be associated with whistlers, and because of the dispersion the waves might last for several seconds. On the ground it is difficult to follow the whistlers to low frequencies, but from satellites, proton whistlers have been measured at frequencies down to ~100 Hz [*Shawhan*, 1966]. However, few studies have addressed this frequency portion of whistlers. In fact, the extent to which waves in the 10- to 100-Hz range occur at high altitudes in the near-equatorial region of outer radiation belt L shells is not well known. These data indicate the need for further measurements of low-frequency waves.

It would have been desirable to have measured the low-frequency wave environment near the equator simultaneously with the particle observations at low altitudes. However, waves at the appropriate position are measured only infrequently, and the probability of having performed such a measurement in coincidence with the rare events reported here is quite low. It is possible that the wave-particle interactions took place at low altitudes, as reported by *Koons et al.* [1972], where the frequency of any responsible waves would be much higher, but low-altitude measurements of the waves were also not available at the times of the events. Lacking one-to-one coordinations between wave and particle measurements, we might compare the times of occurrence of the events with the

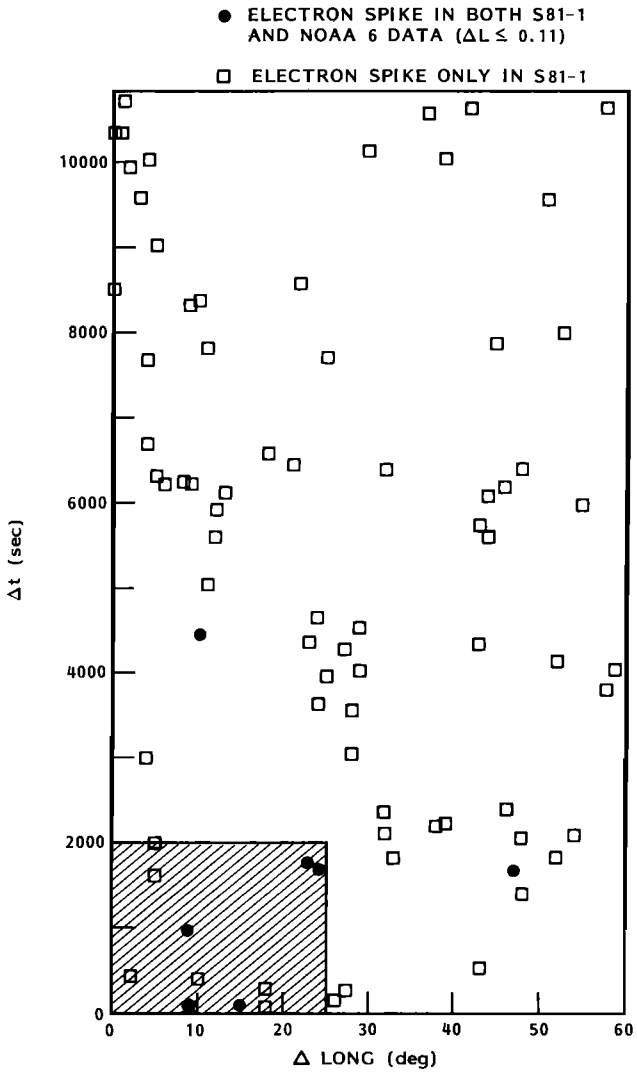

Fig. 8. Differences in longitude and time for events observed in both the S81-1 and the NOAA 6 payloads. The solid circles represent events when a narrow electron spike was observed in both the S81-1 and the NOAA 6 data, but in two of these cases the spike in the NOAA 6 data had an observed duration somewhat greater than 10 s. Five of the seven coincident events are within the shaded box.

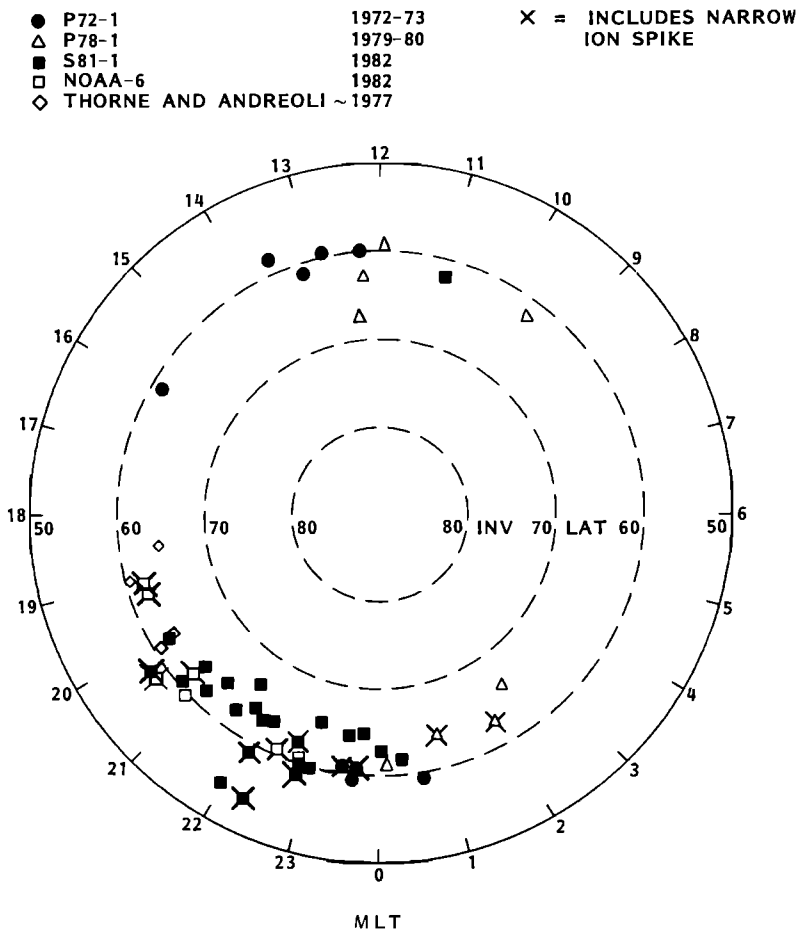

Fig. 9. An invariant latitude/magnetic local time plot of the events observed on the P72-1, the P78-1, and the S81-1 spacecraft as well as the four electromagnetic ion cyclotron wave events reported by *Thorne and Andreoli* [1980]. Events observed on the NOAA 6 spacecraft within 3 hours in time and 0.11 units in L of those measured on the S81-1 satellite are also shown. All of the events from the P72-1, P78-1, and S81-1 vehicles were observed over a period of less than 10 s, as were the proton events from NOAA 6. Two of the electron events measured on NOAA 6 were somewhat longer than 10 s. The principal data coverage was in the MLT intervals 1000–1400 and 2200–0200 on the P72-1 and P78-1 satellites and in the intervals 0830–1230 and 2030–0030 on the S81-1 spacecraft, and for NOAA 6 the range of coverage for low L values was 0630–0900 and 1830–2130.

expected times of the presence of low-frequency waves. *Bossen et al.* [1976] have reported PC 1 events at synchronous orbit to have an increased occurrence rate within $1\frac{3}{4}$ hours of a substorm expansion onset. In Figure 12 the times of the spike events are indicated on plots of the *AE* index. It can be seen that six of the eight events in 1980 occurred very close to the times of substorms and likewise for six of the nine events in 1972–1973. Therefore during many of the events it is likely that low-frequency waves were enhanced in the near-equatorial region.

The narrow L shell confinement of the relativistic precipitation spikes may reflect fine structure in the cold plasma density profiles and hence in the cyclotron resonance energies. Narrow regions of enhanced or depleted plasma density near the plasmapause have been reported by *Anderson* [1984]. Fine structure in the plasma density profiles might also explain the pronounced and narrow depletions of the lower-energy electrons just before and after the spike on November 7, 1980. The nearby spikes in electron and ion precipitation might be attributed to fine spatial structure in the plasma density profiles combined with the presence of waves spanning a sufficiently broad frequency range. Minor displacements in the electron and ion spikes might be attributed to details of the plasma density profiles and the wave intensity-frequency distributions.

In addition to the cyclotron resonance energies being strongly localized, the waves might also be confined to narrow spatial regions. Many years ago it was suggested by *Smith et al.* [1960] that whistler mode waves could be trapped in plasma ducts aligned with the earth's magnetic field lines. Subsequently, observations have supported this concept, and recently, *Beghin et al.* [1984] observed density structures containing ducted waves. These structures were called "ELF plasma ducts." The typical horizontal sizes of these plasma ducts were found to lie in the range 5–50 km. Such dimensions are not inconsistent with the sizes of the spikes reported here, which are typically in the neighborhood of 5 s or ~35-km distance. Plasma densities were measured in the SEEP payload on the S81-1 satellite [*Voss et al.*, 1985], and in several of the passes a density depletion was observed in the plasma trough near the relativistic electron spikes.

SUMMARY

Data have been presented on rare relativistic electron and energetic ion precipitation events with the characteristics of a

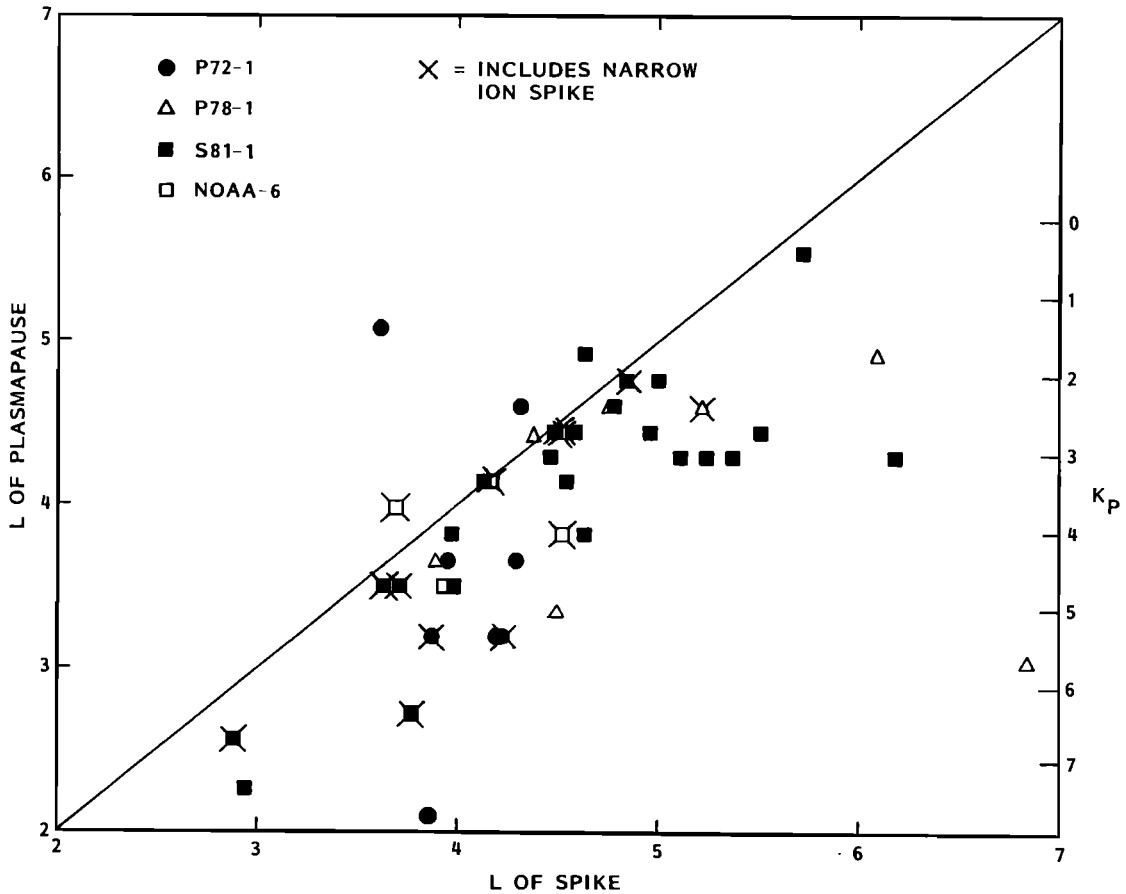

Fig. 10. The locations in L of the preferential high-energy spikes plotted as a function of the plasmapause positions based on Kp [*Carpenter and Park*, 1973]. L of plasmapause is equal to $5.7 - 0.47 \times$ (maximum Kp in previous 12 hours). All of the events from the P72-1, P78-1, and S81-1 vehicles were observed over a period of less than 10 s, as were the proton events from NOAA 6. Two of the electron events measured on NOAA 6 were somewhat longer than 10 s.

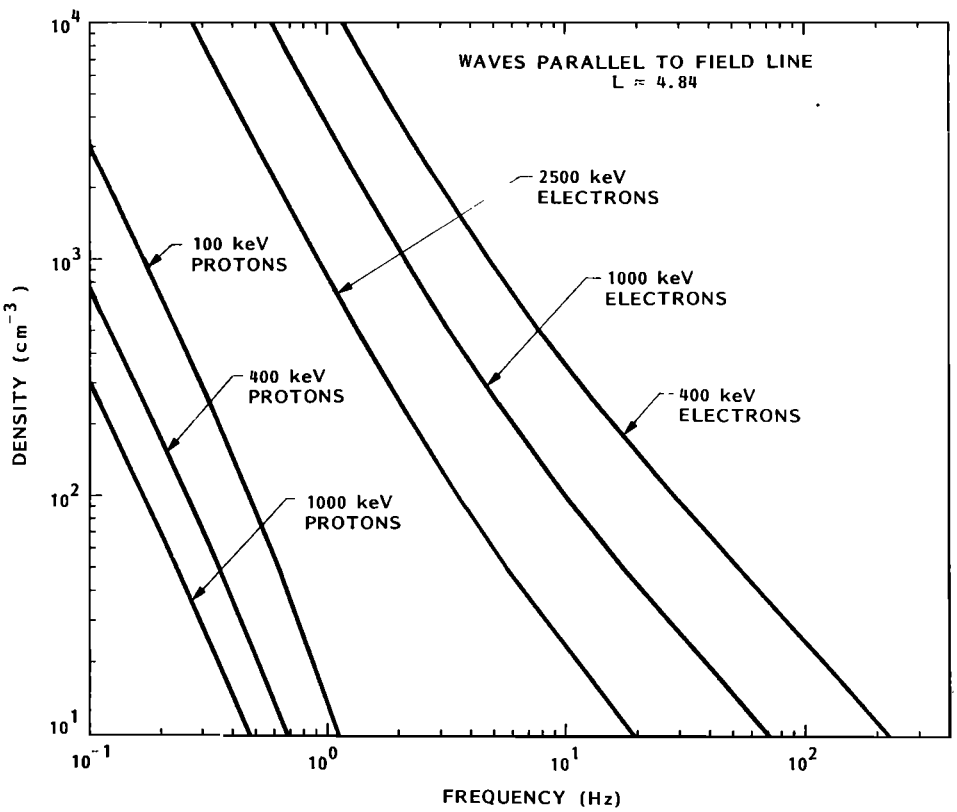

Fig. 11. The calculated resonance frequencies at the equator for electrons and protons of selected energies traveling parallel to the magnetic field line plotted as a function of the near-equatorial cold plasma density. The selected L value corresponds to the spike observed on November 7, 1980. These calculations were performed using a computer program supplied by G. T. Davidson (private communication, 1984).

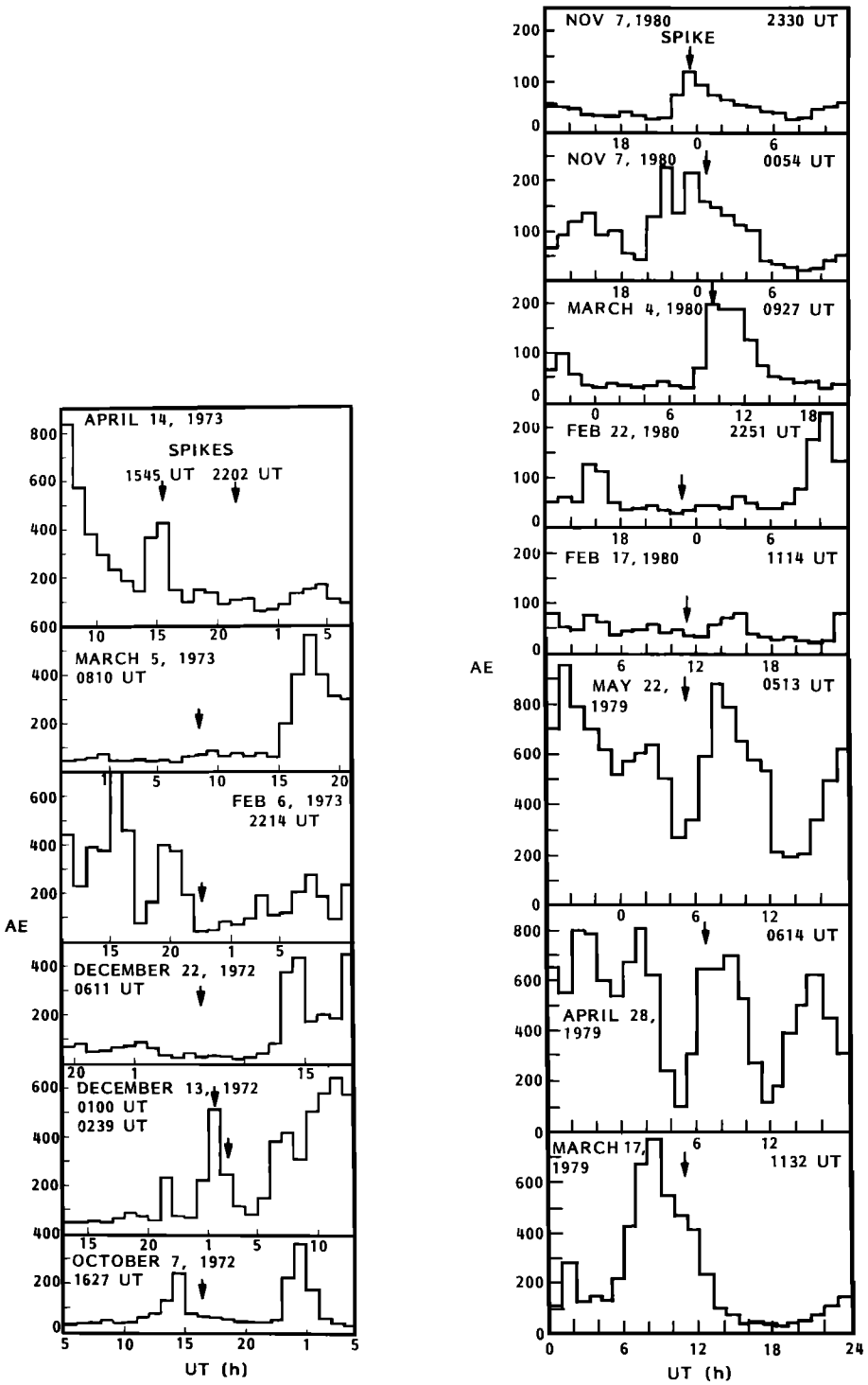

Fig. 12. The *AE* index plotted as a function of time. Arrows indicate the times of the precipitation spike events. The arrow near 0100 UT on December 13, 1972, represents two spike events.

very hard spectrum and narrow spatial extent. The most promising explanation is wave-particle interactions within fine structures in the cold plasma.

Acknowledgments. The development of the P72-1 and P78-1 satellite payloads and the performance of the experiments were supported by the Defense Advanced Research Project Agency through the Office of Naval Research (contracts N00014-69-C-0372 and N00014-78-C-0070, respectively). The SEEP payload on the S81-1 spacecraft was sponsored by the Office of Naval Research (contract N00014-79-C-0824). For all three of these satellite experiments, launch and orbital support were provided by the Air Force Space Test Program Office. Much of the data analysis presented here was sponsored by the Lockheed Independent Research Programs. Appreciation is extended to J. P. McGlennon and C. K. Chalmers for their efforts in processing the data. We also acknowledge the contribution of V. J. Hill, who wrote the program which reduced and archived the NOAA 6 data.

The Editor thanks the two referees for their assistance in evaluating this paper.

REFERENCES

Anderson, R. R., Plasmapause location and structure as deduced from the ISEE 1 plasma wave experiment data (abstract), *Space Res.*, *XXV*, 37, 1984.

Beghin, C., J. C. Cerisier, J. L. Rauch, J. J. Berthelter, F. Lefeuvre, R. Debrie, O. A. Maltseva, and N. I. Massevitch, Experimental evidence of field-aligned ELF plasma ducts in the ionospheric trough and in the auroral zone, paper presented at the International Con-

ference on the Results of the ARCAD 3 Project and of the Recent Programs in Magnetospheric and Ionospheric Physics, Toulouse, France, Centre Natl. d'Etudes Spatiales, Toulouse, France, May 1984.

Bossen, M., R. L. McPherron, and C. T. Russell, A statistical study of Pc 1 magnetic pulsations at synchronous orbit, *J. Geophys. Res.*, *81*, 6083, 1976.

Cain, J. C., S. J. Hendricks, R. A. Langel, and W. V. Hudson, A proposed model for the International Geomagnetic Reference Field, *J. Geomagn. Geolectr.*, *19*, 335, 1967.

Carpenter, D. L., and C. G. Park, On what ionospheric workers should know about the plasmapause-plasmasphere, *Rev. Geophys.*, *11*, 133, 1973.

Davidson, G. T., Relativistic electron precipitation and resonance with ion cyclotron waves, *J. Atmos. Terr. Phys.*, *40*, 1085, 1978.

Imhof, W. L., J. B. Reagan, G. H. Nakano, and E. E. Gaines, Narrow spikes in the selective precipitation of relativistic electrons at mid-latitudes, *J. Geophys. Res.*, *82*, 117, 1977.

Imhof, W. L., J. B. Reagan, G. H. Nakano, and E. E. Gaines, Studies of the sharply defined *L* dependent energy threshold for isotropy at the midnight trapping boundary, *J. Geophys. Res.*, *84*, 6371, 1979.

Imhof, W. L., E. E. Gaines, and J. B. Reagan, Observations of multiple, narrow energy peaks in electrons precipitating from the inner radiation belt and their implications for wave-particle interactions, *J. Geophys. Res.*, *86*, 1591, 1981.

Koons, H. C., Proton precipitation by a whistler-mode wave from a VLF transmitter, *Geophys. Res. Lett.*, *2*, 281, 1975.

Koons, H. C., A. L. Vampola, and D. A. McPherson, Strong pitch-angle scattering of energetic electrons in the presence of electrostatic waves above the ionospheric trough region, *J. Geophys. Res.*, *77*, 1771, 1972.

Nakano, G. H., W. L. Imhof, and R. G. Johnson, A satellite-borne high resolution Ge (Li) gamma-ray spectrometer system, 1, Description of the instruments and gamma-ray backgrounds in earth orbit, *IEEE Trans. Nucl. Sci.*, *21*, 159, 1974.

Nakano, G. H., W. L. Imhof, and J. B. Reagan, High resolution gamma-ray spectroscopy on the P78-1 satellite, *IEEE Trans. Nucl. Sci.*, *27*, 405, 1980.

Reagan, J. B., W. L. Imhof, S. K. Lew, and J. D. Matthews, Observations of quasi-trapped protons at mid latitudes (abstract), *Eos Trans. AGU*, *56*, 1047, 1975.

Shawhan, S. D., Experimental observations of proton whistlers from INJUN 3 VLF data, *J. Geophys. Res.*, *71*, 29, 1966.

Smith, R. L., R. A. Helliwell, and I. W. Yabroff, A theory of trapping of whistlers in field-aligned columns of enhanced ionization, *J. Geophys. Res.*, *65*, 815, 1960.

Thorne, R. M., and L. J. Andreoli, Mechanisms for intense relativistic precipitation, in *Exploration of the Polar Upper Atmosphere, Proceedings of the NATO Advanced Study Institute Held at Lillehammer, Norway*, May 5–16, 1980, p. 381, D. Reidel, Hingham, Mass., 1980.

Thorne, R. M., and C. F. Kennel, Relativistic electron precipitation during magnetic storm main phase, *J. Geophys. Res.*, *76*, 4446, 1971.

Voss, H. D., J. B. Reagan, W. L. Imhof, D. O. Murray, D. A. Simpson, D. P. Cauffman, and J. C. Bakke, Low temperature characteristics of solid state detectors for energetic x-ray, ion, and electron spectrometers, *IEEE Trans. Nucl. Sci.*, *29*, 164, 1982.

Voss, H. D., J. Mobilia, D. W. Datlowe, and S. N. Roselle, The ground support computer and in-orbit survey data analysis program for the SEEP experiment, *IEEE Trans. Nucl. Sci.*, *32*, 168, 1985.

West, R. H., and G. K. Parks, ELF emissions and relativistic electron precipitation, *J. Geophys. Res.*, *89*, 159, 1984.

D. W. Datlowe, E. E. Gaines, W. L. Imhof, J. Mobilia, J. B. Reagan, and H. D. Voss, Lockheed Palo Alto Research Laboratory, Palo Alto, CA 94304.

D. S. Evans, National Oceanic and Atmospheric Administration, Boulder, CO 80303.

(Received August 8, 1985;
revised November 8, 1985;
accepted November 11, 1985.)